

MESH DENOISING AND INPAINTING USING THE TOTAL VARIATION OF THE NORMAL^{*}

Lukas Baumgärtner[†] Ronny Bergmann[‡] Marc Herrmann[§] Roland Herzog[‡]
 Stephan Schmidt[†] José Vidal-Núñez[¶]

In this paper we present a novel approach to solve surface mesh denoising and inpainting problems. The purpose is not only to remove noise while preserving important features such as sharp edges, but also to fill in missing parts of the geometry. A discrete variant of the total variation of the unit normal vector field serves as a regularizing functional to achieve this goal. In order to solve the resulting problem, we present a novel variant of the split Bregman (ADMM) iteration. Numerical examples are included demonstrating the performance of the method with some complex 3D geometries.

Keywords. mesh denoising, mesh inpainting, total variation of the normal vector, split Bregman iteration

This work has been submitted to the IEEE for possible publication. Copyright may be transferred without notice, after which this version may no longer be accessible.

1 INTRODUCTION

Meshes are widely employed in computer graphics and computer vision, where they are utilized to model arbitrary shapes and real geometries. Meshes can be produced by 3D scanners and can be

^{*}This work was supported by DFG grants HE 6077/10-1 and SCHM 3248/2-1 within the Priority Program SPP 1962 (Non-smooth and Complementarity-based Distributed Parameter Systems: Simulation and Hierarchical Optimization), which is gratefully acknowledged.

[†]Institut für Mathematik, Humboldt University of Berlin, 10099 Berlin, Germany (lukas.baumgaertner@hu-berlin.de, <https://www.mathematik.hu-berlin.de/en/people/mem-vz/1693318>, ORCID 0000-0003-1007-4815, s.schmidt@hu-berlin.de, <https://www.mathematik.hu-berlin.de/en/people/mem-vz/1693090>, ORCID 0000-0002-4888-0794).

[‡]Technische Universität Chemnitz, Faculty of Mathematics, 09107 Chemnitz, Germany (ronny.bergmann@mathematik.tu-chemnitz.de, <https://www.tu-chemnitz.de/mathematik/part.dgl/people/bergmann>, ORCID 0000-0001-8342-7218, roland.herzog@mathematik.tu-chemnitz.de, <https://www.tu-chemnitz.de/mathematik/part.dgl/people/herzog>, ORCID 0000-0003-2164-6575).

[§]Julius-Maximilians-Universität Würzburg, Faculty of Mathematics and Computer Science, Lehrstuhl für Mathematik VI, Emil-Fischer-Straße 40, 97074 Würzburg, Germany (no email address provided, <https://www.mathematik.uni-wuerzburg.de/~herrmann>, ORCID 0000-0002-5490-3681).

[¶]University of Alcalá, Department of Physics and Mathematics, 28801 Alcalá de Henares, Spain (j.vidal@uah.es, <https://www.uah.es/es/estudios/profesor/Jose-Vidal-Nunez/>, ORCID 0000-0002-1190-6700).

efficiently processed numerically with appropriate software. Unfortunately, the process of geometry acquisition by scanning leads to unavoidable errors in the form of noise or missing parts. The process of removing such noise while preserving relevant features is known as *mesh denoising*. When missing parts of the geometry must be filled in we speak of *mesh inpainting*.

The aforementioned problems have been of interest in the community of *image processing* since late in the 1980s; see for instance [Caselles, Chambolle, Novaga, 2015](#). Also for mesh denoising, many algorithms exist, and we refer the reader, e.g., to [Botsch et al., 2007](#) for a survey.

Before giving a brief overview of the different types of methods for mesh denoising, we would like to clarify that surface *fairing* (or smoothing) and mesh denoising should be clearly distinguished. The goal of the latter is to remove spurious information from the geometry while preserving sharp features in it, while the goal of the former is to smooth the geometry represented by the mesh with less emphasis on the recovery of edges.

Denoising methods based on diffusion can be classified either as isotropic or anisotropic. They can also often be traced back to perimeter minimization and curvature flows. On the one hand, isotropic methods are applied for mesh fairing and their main characteristic is that they do not take into account the geometric features. As examples of such methods we mention [Field, 1988](#); [Taubin, 1995](#); [Desbrun et al., 1999](#) and [Vollmer, Mencl, Müller, 1999](#). These methods generally have the drawback that they may suffer from surface shrinkage and tend to blur geometric features. On the other hand, anisotropic diffusion methods, as detailed in [Section 2.1](#), can give good recovery results but meshes with sharp edges are still a challenge to them. To overcome this drawback, several approaches have been developed in the literature, as detailed in the following section.

2 RELATED WORK FOR MESH DENOISING

In this section we provide a brief overview of different types of mesh denoising approaches. Since mesh inpainting problems are similar, we do not explicitly discuss specific algorithms for them.

2.1 ANISOTROPIC DIFFUSION

One group of methods for mesh denoising is based on anisotropic diffusion. As their characteristic, these methods take into account feature directions while filtering the normal vector. References [Bajaj, Xu, 2003](#); [Clarenz, Diewald, Rumpf, 2000](#); [Tasdizen et al., 2002](#) and [Hildebrandt, Polthier, 2004](#) fall into this category. Generally speaking, these methods can preserve genuine features such as edges, but they may be numerically unstable during the diffusion process [Zhao et al., 2018](#).

2.2 BILATERAL FILTERING

Bilateral filtering methods are one-stage iterative approaches use the normal and tangential directions to determine a filter at every vertex of the mesh. They then compute a displacement correction for the vertex and update its position. This estimation, however, may be inaccurate due to the presence of noise in the mesh, which may lead to edges not being well preserved. In this category, we mention [Fleishman, Drori, Cohen-Or, 2003](#); [Jones, Durand, Desbrun, 2003](#) where the authors extend the bilateral filter method in imaging processing from [Tomasi, Manduchi, 1998](#) to denoise 3D meshes.

2.3 NORMAL FILTERING AND VERTEX UPDATE

The class of normal filtering and vertex update methods are characterized as two-stage methods whose idea is first to filter the facet normals and subsequently update the vertex positions according to the filtered normals. Nevertheless, they might blur small-scale features since most of them filter facet normals by averaging neighboring (facet) normals. Particular methods of this class differ w.r.t. the treatment of the facet normal vector since the vertex update usually is quite straightforward. Among others, we mention [Ohtake, Belyaev, Seidel, 2002](#); [Sun et al., 2007](#); [Zheng et al., 2011](#); [Zhang et al., 2015](#); [Wang, Fu, et al., 2015](#) and more recently, [Wang, Liu, Tong, 2016](#); [Yadav, Reitebuch, Polthier, 2018](#) and [Centin, Signoroni, 2018](#).

2.4 L_0 MINIMIZATION

Another popular class of methods for mesh denoising is based on the so-called L_0 minimization, mixing both vertex and normal regularization; see [He, Schaefer, 2013](#) and [Zhao et al., 2018](#). The L_0 term introduces sparsity into a discrete gradient operator describing the variation of the surface. One of the weak points of this class of methods is that the non-convexity of the model leads to a high demand in computational resources.

2.5 VERTEX CLASSIFICATION AND DENOISING

Vertex classification and denoising methods can also be understood as two-stage methods since they classify the vertices of the mesh first, and then apply a denoising method per class or cluster of vertices. As examples of such methods we highlight [Wei, Yu, et al., 2015](#); [Lu, Deng, Chen, 2016](#); [Wang, Zhang, Yu, 2012](#); [Zhu et al., 2013](#); [Wei, Liang, et al., 2017](#). Although the idea of separating vertices in homogeneous classes seems to be promising, the presence of noise can make the vertex classification difficult or unreliable; see [Lu, Deng, Chen, 2016](#). As a consequence, this class of methods depends heavily on the level of noise that the mesh has.

2.6 TOTAL VARIATION (TV) FOR MESH DENOISING

We now provide a brief overview over the utility of the total variation semi-norm for mesh denoising. Since the seminal paper [Rudin, Osher, Fatemi, 1992](#), where the so-called ROF model was introduced for image denoising, TV-regularization terms have been heavily utilized in image processing; see [Chan et al., 2006](#); [Chambolle et al., 2010](#) for a good state-of-the-art on TV and its applications. It is well-known that TV-regularizers are especially good at preserving high frequency features in image denoising. Despite this advantage, the total variation based solutions may suffer from the so-called staircasing effect. Moreover, the non-differentiability of the TV-seminorm requires special algorithmic treatment; see for instance the survey [Caselles, Chambolle, Novaga, 2015](#) and the references therein.

To the best of our knowledge, [Tasdizen et al., 2002](#) was the first paper to point out the possibility of applying the idea of total variation for mesh optimization as future research. In [Else, Esedoglu, 2009](#) the authors proposed an analogue of the ROF model based on the Gaussian curvature. The work closest to ours is [Wu et al., 2015](#) where the authors present a variational model for mesh denoising featuring the same TV-regularization term we propose, plus a fairing term. However, they then approximate the TV-seminorm for algorithmic purposes and propose a Euclidean ADMM (alternating direction method of multipliers) to solve the problem.

2.7 OUR CONTRIBUTION AND ORGANIZATION OF THE PAPER

In this paper we present a total variation (TV) approach for mesh reconstruction problems involving mesh denoising and inpainting. While our definition of the TV of the normal agrees with the one in [Wu et al., 2015](#), our algorithmic treatment of the ensuing variational problems is quite different. We employ a differential geometric framework [Lellmann et al., 2013](#) which avoids approximations of the TV term. In fact, a Riemannian version of the ADMM (also known as split Bregman iteration [Goldstein, Osher, 2009](#)) appropriate for this setting was recently proposed in [Bergmann et al., 2020](#); see also [Bergmann et al., 2019](#).

Our contribution here is two-fold. First, we significantly simplify the Riemannian split Bregman iteration compared to [Bergmann et al., 2020](#), and second, we apply it not only to mesh denoising, but also to mesh inpainting problems. The rest of the paper is organized as follows. In [Section 3](#) we review the notion of total variation of the normal vector field. [Section 4](#) is devoted to the derivation of the novel split Bregman iteration and its implementation for mesh denoising problems. In [Section 5](#) we discuss an extension to mesh inpainting. To conclude the paper, in [Section 6](#) we provide a brief summary and identify future research directions.

3 TOTAL VARIATION OF THE NORMAL VECTOR

For the rest of the paper, suppose that Γ is a triangulated surface in \mathbb{R}^3 consisting of flat triangles T , edges E and vertices V . Throughout, we denote vector-valued quantities by bold-face symbols. The authors in [Wu et al., 2015](#) proposed the *total absolute edge-lengthed supplementary angle of the dihedral*

angle (TESA)

$$\sum_E \theta_E |E|_2 \quad (3.1)$$

for surface denoising. Here $|E|_2$ represents the length of the edge E and θ_E is the exterior dihedral angle between two neighboring triangles, i.e., the angle between the respective outward pointing normal vectors. In [Bergmann et al., 2020](#) we proposed the *total variation of the normal*

$$\sum_E |\log_{\mathbf{n}_E^+} \mathbf{n}_E^-|_g |E|_2, \quad (3.2)$$

which can be shown to agree with (3.1). Here the '+' and '-' refer to the two sides of an edge E and $\mathbf{n}_E^+, \mathbf{n}_E^-$ are the outer unit normal vectors of the respective triangles on either side of E . The normal vectors belong to the unit sphere \mathcal{S}^2 in \mathbb{R}^3 . On this manifold, the logarithmic map $\log_{\mathbf{n}_E^+} \mathbf{n}_E^-$ returns the tangent vector pointing from \mathbf{n}_E^+ to \mathbf{n}_E^- and its length $|\log_{\mathbf{n}_E^+} \mathbf{n}_E^-|_g$ equals the geodesic distance (angle) between \mathbf{n}_E^+ and \mathbf{n}_E^- . Since the angle is always non-negative, the functional (3.2) is non-differentiable whenever at least two neighboring normals \mathbf{n}_E^\pm agree. The Riemannian metric $|\cdot|_g$ we use is the pull-back of the Euclidean metric in \mathbb{R}^3 to the tangent space $\mathcal{T}_{\mathbf{n}_E^+} \mathcal{S}^2$ of the unit sphere \mathcal{S}^2 at \mathbf{n}_E^+ .

In this paper, we propose another reformulation of (3.2) which gives rise to a simpler algorithm. It is based on the observation that $\log_{\mathbf{n}_E^+} \mathbf{n}_E^-$ is parallel to the so-called co-normal vector $\boldsymbol{\mu}_E^+$. The latter is the unit vector in the same plane as the triangle T_E^+ , perpendicular to E and outward pointing from T_E^+ ; see [Fig. 3.1](#). Therefore, we obtain

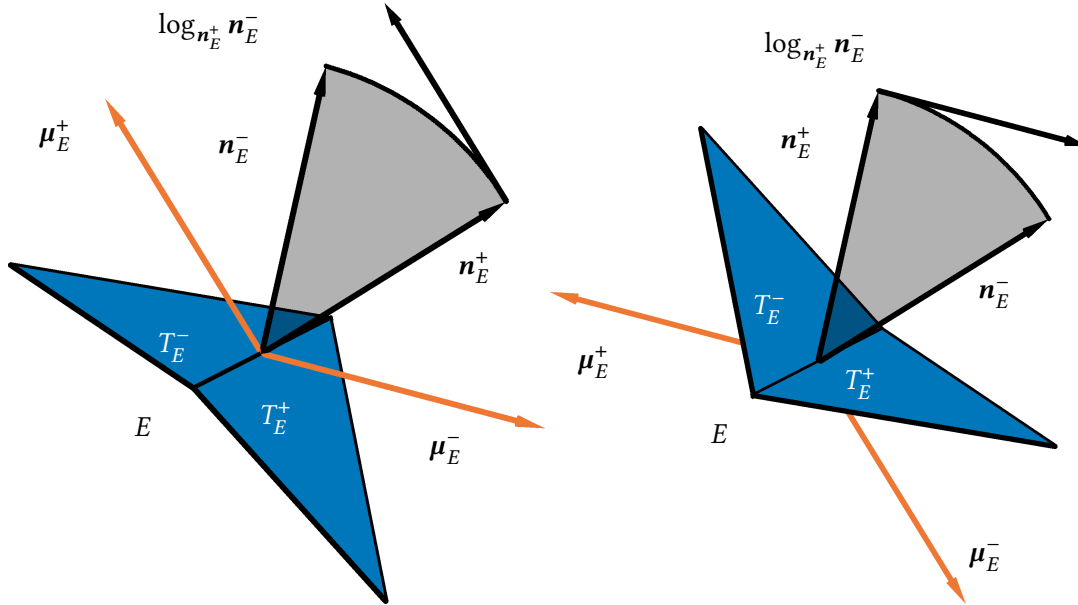


Figure 3.1: Illustration of the geodesic distance (angle) between normals \mathbf{n}_E^+ and \mathbf{n}_E^- and the logarithmic map $\log_{\mathbf{n}_E^+} \mathbf{n}_E^-$ (shown in black) of two triangles T_E^+, T_E^- (shown in blue) which share the edge E . The triangles' co-normals $\boldsymbol{\mu}_E^+$ and $\boldsymbol{\mu}_E^-$ are shown in orange. Notice that $\log_{\mathbf{n}_E^+} \mathbf{n}_E^-$ is parallel to $\boldsymbol{\mu}_E^+$.

$$|\log_{\mathbf{n}_E^+} \mathbf{n}_E^-|_g = |(\log_{\mathbf{n}_E^+} \mathbf{n}_E^-) \cdot \boldsymbol{\mu}_E^+| = \arccos(\mathbf{n}_E^+ \cdot \mathbf{n}_E^-) \quad (3.3)$$

and it is easy to see that

$$(\log_{\mathbf{n}_E^+} \mathbf{n}_E^-) \cdot \boldsymbol{\mu}_E^+ = \text{sign}(\boldsymbol{\mu}_E^+ \cdot \mathbf{n}_E^-) \arccos(\mathbf{n}_E^+ \cdot \mathbf{n}_E^-) \quad (3.4)$$

holds. Compared to the common definition of the discrete total variation semi-norm in imaging, which involves the absolute value of the difference of neighboring function values, the \arccos in (3.3) appears to be highly non-linear. However, it agrees with the geodesic distance and is thus the natural extension of the absolute value of the difference for \mathcal{S}^2 -valued data. In addition, (3.4) can be viewed as the signed distance between neighboring normal vectors.

To illustrate this behaviour, let $\alpha \in (-\pi, \pi)$ be the angle between the normal vectors of two neighbouring triangles T^+ and T^- , such that $\alpha = 0$ refers to the case where the two triangles are co-planar, $\alpha < 0$ represents the concave situation and $\alpha > 0$ the convex one. Without loss of generality, the two normal vectors can be parametrized by

$$\mathbf{n}^+ = (\sin \alpha, \cos \alpha, 0)^\top \quad \text{and} \quad \mathbf{n}^- = (0, 1, 0)^\top,$$

which yields

$$\boldsymbol{\mu}^+ = (-\cos \alpha, \sin \alpha, 0)^\top.$$

Then (3.3) is simplified to

$$\arccos(\mathbf{n}^+ \cdot \mathbf{n}^-) = \arccos(\cos \alpha) = |\alpha|$$

and (3.4) becomes

$$\text{sign}(\boldsymbol{\mu}^+ \cdot \mathbf{n}^-) \arccos(\mathbf{n}^+ \cdot \mathbf{n}^-) = \text{sign}(\sin \alpha) |\alpha| = \alpha.$$

In the following section, we employ functional (3.2) as a prior in different shape optimization problems and solve these with the split Bregman method. To this end, we have to differentiate the expression

$$\text{sign}(\boldsymbol{\mu}^+ \cdot \mathbf{n}^-) \arccos(\mathbf{n}^+ \cdot \mathbf{n}^-) \quad (3.5)$$

with respect to the shape, i.e., with respect to the vertex positions of the triangles involved. Notice that \mathbf{n}^+ , \mathbf{n}^- and $\boldsymbol{\mu}^+$ all depend smoothly on the vertex positions. Therefore, in order to demonstrate the differentiability of (3.5), it is sufficient to differentiate with respect to \mathbf{n}^+ , \mathbf{n}^- and $\boldsymbol{\mu}^+$, and apply the chain rule afterwards. Due to the jump of sign, we exclude the case $\mathbf{n}^+ = \mathbf{n}^-$ for now. Then the derivative of $\text{sign}(\boldsymbol{\mu}^+ \cdot \mathbf{n}^-)$ w.r.t. all three quantities is zero and its dependency on the shape can be ignored when differentiating (3.5).

The derivative of $\arccos(\mathbf{n}^+ \cdot \mathbf{n}^-)$ with respect to $\mathbf{n}^+ \in \mathcal{S}^2$ reads

$$\frac{\partial \arccos(\frac{\mathbf{n}^+}{|\mathbf{n}^+|_g} \cdot \mathbf{n}^-)}{\partial \mathbf{n}^+} = \frac{-(|\mathbf{n}^+|_g \mathbf{n}^- - (\mathbf{n}^+ \cdot \mathbf{n}^-) \frac{\mathbf{n}^+}{|\mathbf{n}^+|_g})}{\sqrt{1 - (\mathbf{n}^+ \cdot \mathbf{n}^-)^2} |\mathbf{n}^+|_g^2} = \frac{-(\mathbf{n}^- - (\mathbf{n}^+ \cdot \mathbf{n}^-) \mathbf{n}^+)}{\sqrt{1 - (\mathbf{n}^+ \cdot \mathbf{n}^-)^2}}. \quad (3.6)$$

A simple calculation shows that this resulting vector is normalized and the numerator is parallel to $\boldsymbol{\mu}^+$. Proceeding similarly for the derivative with respect to \mathbf{n}^- , we can summarize our findings as

$$\begin{aligned} \frac{\partial \text{sign}(\boldsymbol{\mu}^+ \cdot \mathbf{n}^-) \arccos(\frac{\mathbf{n}^+}{|\mathbf{n}^+|_g} \cdot \mathbf{n}^-)}{\partial \mathbf{n}^+} &= -\boldsymbol{\mu}^+, \\ \frac{\partial \text{sign}(\boldsymbol{\mu}^+ \cdot \mathbf{n}^-) \arccos(\frac{\mathbf{n}^-}{|\mathbf{n}^-|_g} \cdot \mathbf{n}^+)}{\partial \mathbf{n}^-} &= -\boldsymbol{\mu}^-. \end{aligned} \quad (3.7)$$

From here we also infer that the assumption $\mathbf{n}^+ \neq \mathbf{n}^-$ is no longer necessary, since both expressions in (3.7) are continuous even across $\mathbf{n}^+ = \mathbf{n}^-$.

4 MESH DENOISING PROBLEM

In this section we consider an analogue of the ROF model for mesh denoising. The vertex positions $\mathbf{x}_V \in \mathbb{R}^3$ serve as optimization variables, and they implicitly determine the triangles' normal and co-normal vectors. Using the reformulation (3.3), we consider the following variational model:

$$\text{Minimize } \frac{1}{2} \sum_V |\mathbf{x}_V - \mathbf{x}_V^{\text{data}}|_2^2 + \beta \sum_E |(\log_{\mathbf{n}_E^+} \mathbf{n}_E^-) \cdot \boldsymbol{\mu}_E^+| |E|_2. \quad (4.1)$$

Here $\mathbf{x}_V^{\text{data}} \in \mathbb{R}^3$ are the given, noisy vertex positions which serve as data in the fidelity term in (4.1).

To solve this problem, we apply a variant of the split Bregman method [Goldstein, Osher, 2009](#). To this end, we introduce the additional variable $d_E = (\log_{\mathbf{n}_E^+} \mathbf{n}_E^-) \cdot \boldsymbol{\mu}_E^+$ and let b_E the associated (scaled) Lagrange multiplier.

Summarizing the unknowns \mathbf{x}_V , d_E and b_E into vectors, the associated augmented Lagrangian reads

$$\mathcal{L}(\mathbf{x}, d, b) := \frac{1}{2} \sum_V |\mathbf{x}_V^{\text{data}} - \mathbf{x}_V|_2^2 + \beta \sum_E |d_E| |E|_2 + \frac{\lambda}{2} \sum_E [d_E - (\log_{\mathbf{n}_E^+} \mathbf{n}_E^-) \cdot \boldsymbol{\mu}_E^+ - b_E]^2 |E|_2. \quad (4.2)$$

Split Bregman iterations are characterized by the fact that \mathcal{L} is minimized iteratively independently with respect to \mathbf{x} and d , respectively, and subsequently an update of the Lagrange multiplier b is performed. We now discuss these subproblems.

The \mathbf{x} -problem, i.e., the minimization of (4.2) w.r.t. all vertex positions \mathbf{x}_V , can be thought of as a discrete shape optimization problem. Notice that $|E|_2$, $\log_{\mathbf{n}_E^+} \mathbf{n}_E^-$ and $\boldsymbol{\mu}_E^+$ depend in a nonlinear but smooth way on \mathbf{x} as long as all triangles maintain positive area, which we ensure. In our implementation, we utilize the algorithmic differentiation capabilities of FENICS [Alnæs et al., 2015](#); [Logg, Mardal, Wells, 2012](#) in order to obtain the total derivative of $\mathcal{L}(\mathbf{x}, d, b)$ w.r.t. the vector \mathbf{x} of vertex positions. Rather than to minimize (4.2) exactly, we only perform a few shape gradient steps.

The d -problem is non-smooth, but it completely decouples, and the problem on each edge is well known to have a closed-form solution expressed in terms of the shrinkage operator, namely

$$d_E = \max \{ |v_E| - \beta \lambda^{-1}, 0 \} \text{sign}(v_E), \quad (4.3)$$

where $v_E = (\log_{\mathbf{n}_E^+} \mathbf{n}_E^-) \cdot \boldsymbol{\mu}_E^+ + b_E$. Finally, the update for the Lagrange multiplier is simply given by $b_E \leftarrow b_E + (\log_{\mathbf{n}_E^+} \mathbf{n}_E^-) \cdot \boldsymbol{\mu}_E^+ - d_E$. For completeness, our split Bregman method for (4.1) is summarized in [Algorithm 1](#).

Let us briefly discuss the differences to the Riemannian split Bregman method for (4.1) recently proposed in [Bergmann et al., 2020](#). In the latter, the alternative splitting $\hat{\mathbf{d}}_E = \log_{\mathbf{n}_E^+} \mathbf{n}_E^- \in \mathcal{T}_{\mathbf{n}_E^+} \mathcal{S}^2$ was used, which required the Lagrange multiplier estimate $\hat{\mathbf{b}}_E$ to also belong to $\mathcal{T}_{\mathbf{n}_E^+} \mathcal{S}^2$. Although $\hat{\mathbf{d}}_E$ can still be expressed explicitly in terms of a (vectorial) shrinkage operation, the multiplier estimate needs to be parallelly transported once per iteration into the new tangent space $\mathcal{T}_{\mathbf{n}_E^+} \mathcal{S}^2$ after the geometry update (which entails an update of the normal vectors). We refer the reader to [Bergmann et al., 2020](#),

Algorithm 3.1 for details. This parallel transport, although computable by an explicit formula, is the most costly step. By contrast, our new Algorithm 1 is simpler and it involves only a scalar shrinkage for d_E and, most importantly, does not require the parallel transport step for the Lagrange multiplier estimate.

Fig. 4.1 shows a denoising result obtained using the model (4.1) and Algorithm 1 after 200 outer iterations, while performing one gradient step with step length 0.01 per outer iteration. The data $\mathbf{x}_V^{\text{data}}$ is from the well-known *fandisk* benchmark problem, where noise was added to each vertex. The noise at a vertex is added in normal direction using a Gaussian distribution with standard deviation $\sigma = 0.3$ times the average length of all edges. Our implementation was done in FENICS (version 2018.2.devo).

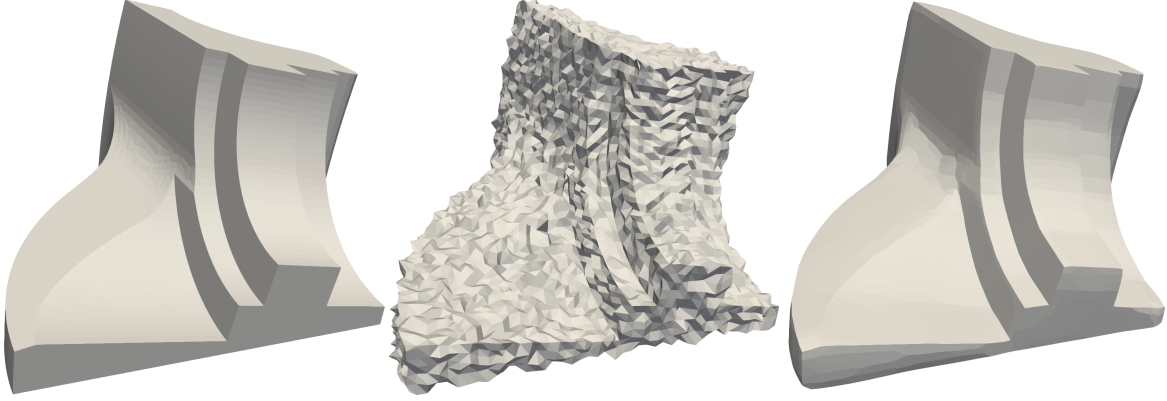


Figure 4.1: Mesh denoising using the split Bregman iteration on (4.1) with $\beta = 0.01$, $\lambda = 0.1$. Original geometry (left), noisy geometry (middle) and reconstruction (right).

The same procedure is performed on the Stanford bunny mesh, a less regular object. Numerical results for two different values of β are presented in Fig. 4.2 .

Algorithm 1 Split Bregman method for (4.1)

Require: noisy vertex positions X_V

Ensure: approx. solution of (4.1) with vertex positions \mathbf{x}_V

- 1: Set $b^{(0)} := 0$ and $d^{(0)} := 0$
 - 2: Set $k := 0$
 - 3: **while** not converged **do**
 - 4: Perform one or several gradient steps for $\mathbf{x} \mapsto \mathcal{L}(\mathbf{x}, d^{(k)}, b^{(k)})$ with initial guess $\mathbf{x}^{(k)}$, to obtain $\mathbf{x}^{(k+1)}$ and updated values for the edge lengths $|E|_2$, normal vectors \mathbf{n}_E and co-normal vectors $\boldsymbol{\mu}_E$
 - 5: Set $d^{(k+1)} := \arg \min \mathcal{L}(\mathbf{x}^{(k+1)}, d^{(k)}, b^{(k)})$, see (4.3)
 - 6: Set $b_E^{(k+1)} := b_E^{(k)} + (\log_{\mathbf{n}_E^+} \mathbf{n}_E^-) \cdot \boldsymbol{\mu}_E^+ - d_E^{(k+1)}$ for all edges E
 - 7: Set $k := k + 1$
 - 8: **end while**
-

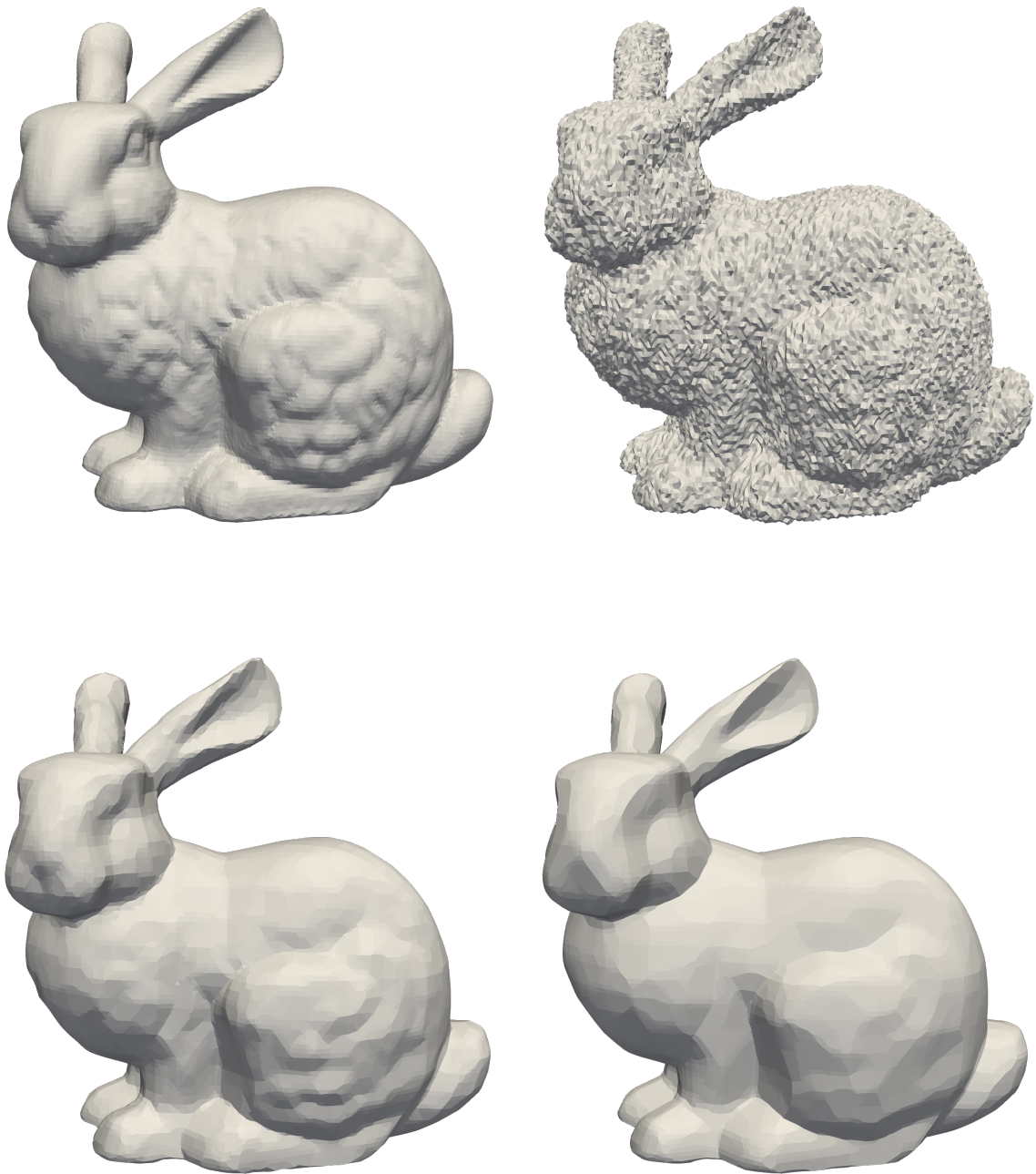


Figure 4.2: Mesh denoising using the split Bregman iteration on (4.1). Original geometry (top left), noisy geometry (top right), reconstruction with $\beta = 0.003$, $\lambda = 0.01$ (bottom left) and with $\beta = 0.01$, $\lambda = 0.01$ (bottom right).

5 MESH INPAINTING PROBLEM

This section is devoted to mesh inpainting problems. These problems differ from (4.1) in that there is no fidelity term. Instead, the exact positions of a number of vertices are given and not subject to noise, while the positions of the remaining vertices are unknown and there is no reference value known for them. In this setting, the augmented Lagrangian (4.2) is replaced by

$$\mathcal{L}(\mathbf{x}, d, b) := \beta \sum_E |d_E| |E|_2 + \frac{\lambda}{2} \sum_E [d_E - (\log_{\mathbf{n}_E^+} \mathbf{n}_E^-) \cdot \boldsymbol{\mu}_E^+ - b_E]^2 |E|_2. \quad (5.1)$$

In contrast to (4.1), the minimization w.r.t. \mathbf{x} is carried out only for the vertices inside the inpainting region while the positions of the remaining vertices are fixed. Note that we need to construct an initial mesh on the inpainting subdomain before running [Algorithm 1](#).

As a first test we consider a unit cube mesh with $10 \times 10 \times 2$ triangles on each side. We select a subdomain on which we simulate the loss of data. We do so by solving a surface area minimization problem on this subdomain, which then solves as the initial guess for the subsequent split Bregman method based on (5.1). We optionally also remesh the subdomain in order to remove any information from the original, intact geometry. Remeshing was performed using the open source software GMSH (version 3.0.6). The inpainting results obtained using FENICS, once starting from the original and once from the newly generated mesh, are shown in [Fig. 5.1](#).

Our algorithm yields different inpainting results, depending on the connectivity of the starting mesh. When using the original connectivity (no remeshing), the original cube was fully recovered. With remeshing, a result was found with one of the corners chopped off; see the bottom right of [Fig. 5.1](#). In fact, the cube with the missing corner has a smaller value of the total variation of the normal than the original one. However, given the connectivity of the mesh, both are local minima to their respective problems.

To show the performance of our algorithm, another inpainting problem is solved on the more complex geometry *fandisk*, with remeshing of the inpainting subdomain. The corresponding results are shown in [Fig. 5.2](#).

6 CONCLUSION

In this paper we introduced a new formulation of the *total variation of the normal* functional equivalent to previous expressions. The new formulation leads to a simplified variant of the previously proposed Riemannian split Bregman algorithm. Specifically, the relatively costly step of parallel transport of the Lagrange multiplier estimate can be avoided. We demonstrate the novel algorithm using mesh denoising and mesh inpainting problems.

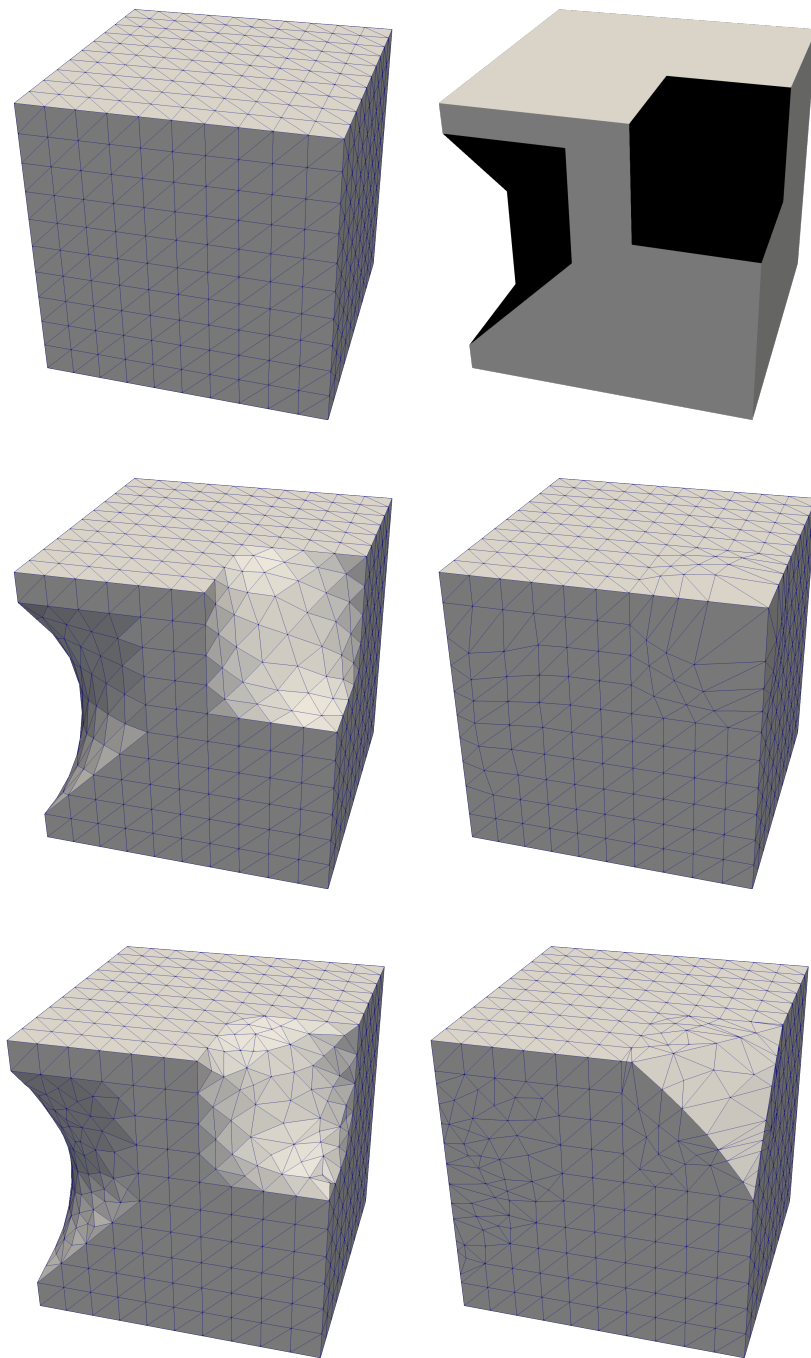


Figure 5.1: Mesh inpainting using the split Bregman iteration for mesh inpainting, based on (5.1) with $\beta = 0.01$, $\lambda = 0.1$. Original mesh (top left) and visualization of the missing parts by painting the inside of the cube black (top right), starting mesh with original mesh connectivity (middle left) and corresponding reconstruction (middle right), previous starting mesh after remeshing with GMSH (bottom left) and corresponding reconstruction (bottom right).

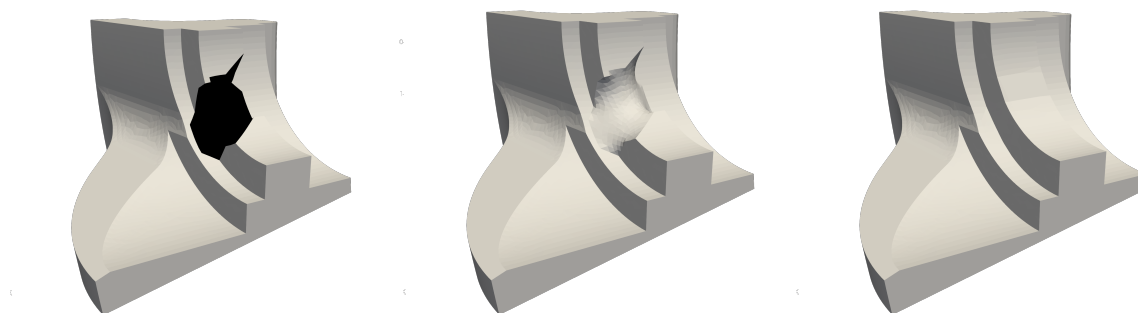


Figure 5.2: Mesh inpainting using the split Bregman iteration for mesh inpainting, based on (5.1) with $\beta = 0.01$, $\lambda = 0.1$, after an initial remeshing was done on the affected area. Visualization of the missing parts by painting the inside black (left), starting mesh obtained by solving a minimal surface problem (middle), and reconstruction (right).

REFERENCES

- Alnæs, M.; J. Blechta; J. Hake; A. Johansson; B. Kehlet; A. Logg; C. Richardson; J. Ring; M. E. Rognes; G. N. Wells (2015). “The FEniCS project version 1.5”. *Archive of Numerical Software* 3.100, pp. 9–23. DOI: [10.11588/ans.2015.100.20553](https://doi.org/10.11588/ans.2015.100.20553).
- Bajaj, C. L.; G. Xu (2003). “Anisotropic diffusion of surfaces and functions on surfaces”. *ACM Transactions on Graphics* 22.1, pp. 4–32. DOI: [10.1145/588272.588276](https://doi.org/10.1145/588272.588276).
- Bergmann, R.; M. Herrmann; R. Herzog; S. Schmidt; J. Vidal-Núñez (2019). “Geometry processing problems using the total variation of the normal vector field”. *Proceedings in Applied Mathematics and Mechanics* 19.1. DOI: [10.1002/pamm.201900189](https://doi.org/10.1002/pamm.201900189).
- Bergmann, R.; M. Herrmann; R. Herzog; S. Schmidt; J. Vidal-Núñez (2020). “Discrete total variation of the normal vector field as shape prior with applications in geometric inverse problems”. *Inverse Problems* 36.5, p. 054003. DOI: [10.1088/1361-6420/ab6d5c](https://doi.org/10.1088/1361-6420/ab6d5c).
- Botsch, M.; M. Pauly; L. Kobbelt; P. Alliez; B. Lévy; S. Bischoff; C. Rössl (2007). “Geometric modeling based on polygonal meshes”. *ACM SIGGRAPH 2007 Courses*. SIGGRAPH ’07. ACM. DOI: [10.1145/1281500.1281640](https://doi.org/10.1145/1281500.1281640).
- Caselles, V.; A. Chambolle; M. Novaga (2015). “Total variation in imaging”. *Handbook of Mathematical Methods in Imaging*. Ed. by O. Scherzer. Springer New York, pp. 1455–1499. DOI: [10.1007/978-1-4939-0790-8_23](https://doi.org/10.1007/978-1-4939-0790-8_23).
- Centin, M.; A. Signoroni (2018). “Mesh denoising with (geo)metric fidelity”. *IEEE Transactions on Visualization and Computer Graphics* 24.8, pp. 2380–2396. DOI: [10.1109/tvcg.2017.2731771](https://doi.org/10.1109/tvcg.2017.2731771).
- Chambolle, A.; V. Caselles; D. Cremers; M. Novaga; T. Pock (2010). “An introduction to total variation for image analysis”. *Theoretical Foundations and Numerical Methods for Sparse Recovery*. Vol. 9. Radon Series on Computational and Applied Mathematics. Walter de Gruyter, Berlin, pp. 263–340. DOI: [10.1515/9783110226157.263](https://doi.org/10.1515/9783110226157.263).
- Chan, T.; S. Esedoglu; F. Park; A. Yip (2006). “Total variation image restoration: overview and recent developments”. *Handbook of Mathematical Models in Computer Vision*. Springer, New York, pp. 17–31. DOI: [10.1007/0-387-28831-7_2](https://doi.org/10.1007/0-387-28831-7_2).
- Clarenz, U.; U. Diewald; M. Rumpf (2000). “Nonlinear anisotropic diffusion in surface processing”. *Visualization*. Ed. by B. H. T. Ertl; A. Varshney, pp. 397–405. DOI: [10.1109/visual.2000.885721](https://doi.org/10.1109/visual.2000.885721).

- Desbrun, M.; M. Meyer; P. Schröder; A. H. Barr (1999). “Implicit fairing of irregular meshes using diffusion and curvature flow”. *Proceedings of the 26th Annual Conference on Computer Graphics and Interactive Techniques*. SIGGRAPH ’99, pp. 317–324. DOI: [10.1145/311535.311576](https://doi.org/10.1145/311535.311576).
- Else, M.; S. Esedoglu (2009). “Analogue of the total variation denoising model in the context of geometry processing”. *Multiscale Modeling & Simulation. A SIAM Interdisciplinary Journal* 7.4, pp. 1549–1573. DOI: [10.1137/080736612](https://doi.org/10.1137/080736612).
- Field, D. A. (1988). “Laplacian smoothing and Delaunay triangulations”. *Communications in Applied Numerical Methods* 4.6, pp. 709–712. DOI: [10.1002/cnm.1630040603](https://doi.org/10.1002/cnm.1630040603).
- Fleishman, S.; I. Drori; D. Cohen-Or (2003). “Bilateral mesh denoising”. *ACM Transactions on Graphics* 22.3, pp. 950–953. DOI: [10.1145/882262.882368](https://doi.org/10.1145/882262.882368).
- Goldstein, T.; S. Osher (2009). “The split Bregman method for L_1 -regularized problems”. *SIAM Journal on Imaging Sciences* 2.2, pp. 323–343. DOI: [10.1137/080725891](https://doi.org/10.1137/080725891).
- He, L.; S. Schaefer (2013). “Mesh denoising via L_0 minimization”. *ACM Transactions on Graphics* 32.4, 64:1–64:8. DOI: [10.1145/2461912.2461965](https://doi.org/10.1145/2461912.2461965).
- Hildebrandt, K.; K. Polthier (2004). “Anisotropic filtering of non-linear surface features”. *Computer Graphics Forum* 23.3, pp. 391–400. DOI: [10.1111/j.1467-8659.2004.00770.x](https://doi.org/10.1111/j.1467-8659.2004.00770.x).
- Jones, T. R.; F. Durand; M. Desbrun (2003). “Non-iterative, feature-preserving mesh smoothing”. *ACM Transactions on Graphics* 22.3, pp. 943–949. DOI: [10.1145/882262.882367](https://doi.org/10.1145/882262.882367).
- Lellmann, J.; E. Strekalovskiy; S. Koetter; D. Cremers (2013). “Total variation regularization for functions with values in a manifold”. *IEEE ICCV 2013*, pp. 2944–2951. DOI: [10.1109/ICCV.2013.366](https://doi.org/10.1109/ICCV.2013.366).
- Logg, A.; K.-A. Mardal; G. N. Wells, eds. (2012). *Automated Solution of Differential Equations by the Finite Element Method*. Springer. DOI: [10.1007/978-3-642-23099-8](https://doi.org/10.1007/978-3-642-23099-8).
- Lu, X.; Z. Deng; W. Chen (2016). “A robust scheme for feature-preserving mesh denoising”. *IEEE Transactions on Visualization and Computer Graphics* 22.3, pp. 1181–1194. DOI: [10.1109/TVCG.2015.2500222](https://doi.org/10.1109/TVCG.2015.2500222).
- Ohtake, Y.; A. Belyaev; H.-P. Seidel (2002). “Mesh smoothing by adaptive and anisotropic Gaussian filter applied to mesh normals”. *7th International Fall Workshop on Vision, Modeling, and Visualization, VMV 2002, Erlangen, Germany, November 20–22, 2002*. Vol. 2, pp. 203–210.
- Rudin, L. I.; S. Osher; E. Fatemi (1992). “Nonlinear total variation based noise removal algorithms”. *Physica D* 60.1–4, pp. 259–268. DOI: [10.1016/0167-2789\(92\)90242-F](https://doi.org/10.1016/0167-2789(92)90242-F).
- Sun, X.; P. Rosin; R. Martin; F. Langbein (2007). “Fast and effective feature-preserving mesh denoising”. *IEEE Transactions on Visualization and Computer Graphics* 13.5, pp. 925–938. DOI: [10.1109/TVCG.2007.1065](https://doi.org/10.1109/TVCG.2007.1065).
- Tasdizen, T.; R. Whitaker; P. Burchard; S. Osher (2002). “Geometric surface smoothing via anisotropic diffusion of normals”. *Visualization, 2002. VIS 2002. IEEE*, pp. 125–132. DOI: [10.1109/VISUAL.2002.1183766](https://doi.org/10.1109/VISUAL.2002.1183766).
- Taubin, G. (1995). “A signal processing approach to fair surface design”. *Proceedings of the 22nd Annual Conference on Computer Graphics and Interactive Techniques*. SIGGRAPH ’95. ACM, pp. 351–358. DOI: [10.1145/218380.218473](https://doi.org/10.1145/218380.218473).
- Tomasi, C.; R. Manduchi (1998). “Bilateral filtering for gray and color images”. *Proceedings of the Sixth International Conference on Computer Vision*. ICCV ’98. IEEE Computer Society. DOI: [10.1109/iccv.1998.710815](https://doi.org/10.1109/iccv.1998.710815).
- Vollmer, J.; R. Mencl; H. Müller (1999). “Improved Laplacian smoothing of noisy surface meshes”. *Computer Graphics Forum* 18.3, pp. 131–138. DOI: [10.1111/1467-8659.00334](https://doi.org/10.1111/1467-8659.00334).
- Wang, J.; X. Zhang; Z. Yu (2012). “A cascaded approach for feature-preserving surface mesh denoising”. *Computer-Aided Design* 44.7, pp. 597–610. DOI: [10.1016/j.cad.2012.03.001](https://doi.org/10.1016/j.cad.2012.03.001).

- Wang, P.-S.; X.-M. Fu; Y. Liu; X. Tong; S.-L. Liu; B. Guo (2015). "Rolling guidance normal filter for geometric processing". *ACM Transactions on Graphics* 34.6, 173:1–173:9. DOI: [10.1145/2816795.2818068](https://doi.org/10.1145/2816795.2818068).
- Wang, P.-S.; Y. Liu; X. Tong (2016). "Mesh denoising via cascaded normal regression". *ACM Transactions on Graphics* 35.6, 232:1–232:12. DOI: [10.1145/2980179.2980232](https://doi.org/10.1145/2980179.2980232).
- Wei, M.; L. Liang; W. Pang; J. Wang; W. Li; H. Wu (2017). "Tensor voting guided mesh denoising". *IEEE Transactions on Automation Science and Engineering* 14.2, pp. 931–945. DOI: [10.1109/TASE.2016.2553449](https://doi.org/10.1109/TASE.2016.2553449).
- Wei, M.; J. Yu; W. M. Pang; J. Wang; J. Qin; L. Liu; P. A. Heng (2015). "Bi-normal filtering for mesh denoising". *IEEE Transactions on Visualization and Computer Graphics* 21.1, pp. 43–55. DOI: [10.1109/tvcg.2014.2326872](https://doi.org/10.1109/tvcg.2014.2326872).
- Wu, X.; J. Zheng; Y. Cai; C.-W. Fu (2015). "Mesh denoising using extended ROF model with L1 fidelity". *Computer Graphics Forum* 34.7, pp. 35–45. DOI: [10.1111/cgf.12743](https://doi.org/10.1111/cgf.12743).
- Yadav, S. K.; U. Reitebuch; K. Polthier (2018). "Mesh denoising based on normal voting tensor and binary optimization". *IEEE Transactions on Visualization and Computer Graphics* 24.8, pp. 2366–2379. DOI: [10.1109/tvcg.2017.2740384](https://doi.org/10.1109/tvcg.2017.2740384).
- Zhang, W.; B. Deng; J. Zhang; S. Bouaziz; L. Liu (2015). "Guided mesh normal filtering". *Computer Graphics Forum* 34.7, pp. 23–34. DOI: [10.1111/cgf.12742](https://doi.org/10.1111/cgf.12742).
- Zhao, Y.; H. Qin; X. Zeng; J. Xu; J. Dong (2018). "Robust and effective mesh denoising using Lo sparse regularization". *Computer-Aided Design* 101, pp. 82–97. DOI: [10.1016/j.cad.2018.04.001](https://doi.org/10.1016/j.cad.2018.04.001).
- Zheng, Y.; H. Fu; O. K.-C. Au; C.-L. Tai (2011). "Bilateral normal filtering for mesh denoising". *IEEE Transactions on Visualization and Computer Graphics* 17.10, pp. 1521–1530. DOI: [10.1109/TVCG.2010.264](https://doi.org/10.1109/TVCG.2010.264).
- Zhu, L.; M. Wei; J. Yu; W. Wang; J. Qin; P.-A. Heng (2013). "Coarse-to-fine normal filtering for feature-preserving mesh denoising based on isotropic subneighborhoods". *Computer Graphics Forum* 32.7, pp. 371–380. DOI: [10.1111/cgf.12245](https://doi.org/10.1111/cgf.12245).